

STATUS OF THE APS DIAGNOSTICS UNDULATOR BEAMLINE

B. X. Yang, A. H. Lumpkin, G. A. Goeppner, S. Sharma, E. Rotela, I. C. Sheng, E. Moog
 Argonne National Lab, 9700 South Cass Avenue, Argonne, IL 60439, USA

Abstract

We report the status of the diagnostics undulator beamline for the Advanced Photon Source (APS) storage ring. The beamline was designed for the characterization of the 7-GeV, low-emittance positron beam at high resolution. The special diagnostics undulator has been manufactured by STI Optronics. The device exhibits very low magnetic field errors at closed gap of 10.5 mm: first field integral less than 15 gauss-cm, and optical phase error less than 1.5°. The front end of the beamline and a monochromator are installed and tested for use on divergence and directional stability measurements with a target resolution of 3 μ rad utilizing the first harmonic radiation of 25 keV. Initial results for the divergence measurement show that the storage ring is operating well within its design goals.

1 INTRODUCTION

For the high energy third-generation synchrotron radiation sources where the particle beam emittance still determines the x-ray beam brilliance, the narrow cone of undulator radiation provides an efficient method to characterize the particle beam divergence and directional stability [1,2].

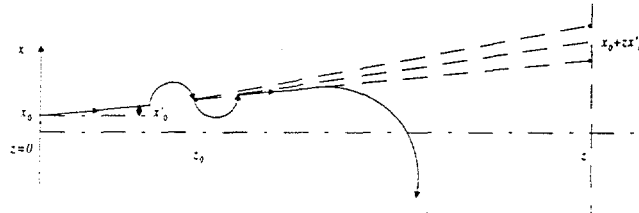


Figure 1: Schematics showing the undulator radiation cone from an off-axis particle: solid line is the particle trajectory and dashed line is the cone of undulator radiation.

Figure 1 illustrates the basic principle for an undulator to be used for particle beam divergence measurements. The undulator is located z_0 from the particle beam waist. A monochromator/detector combination is used at z to measure the x-ray beam profile. If we set the monochromator to select only the photons slightly above the harmonic energy, the observed profile of the x-ray beam generated by a particle with phase space coordinates (x_0, x'_0) can then be approximated by a Gaussian function centered at $x_0 + z x'_0$, with a width of $(z - z_0) \sigma_{p0}$, where the natural undulator beam divergence is approximately

$$\sigma_{p0} \equiv \sqrt{\frac{\lambda}{2L}}. \quad (1)$$

Summing over all particles in the Gaussian beam with widths of (σ_x, σ'_x) , the total rms width of the (monochromatic) x-ray beam cross section is given by the quadrature sum,

$$\Sigma_x^2 = \sigma_x^2 + z^2 \sigma'^2 + (z - z_0)^2 \sigma_{p0}^2. \quad (2)$$

The size and the divergence at the beam waist is further related to the emittance ϵ_x and the beta function β_x ,

$$\sigma_x = \sqrt{\beta_x \epsilon_x} \text{ and } \sigma'_x = \sqrt{\frac{\epsilon_x}{\beta_x}}. \quad (3)$$

Hence we have

$$\epsilon_x = \beta_x \frac{\Sigma_x^2 - (z - z_0)^2 \sigma_{p0}^2}{\beta_x^2 + z^2}. \quad (4)$$

When $z = z_0$, this formula takes the form given in Ref. 1. Table 1 shows the design parameters of the APS storage ring insertion straight section. While the 10% vertical coupling was the baseline design goal, 1% and 0.1% coupling represents the upgrade path of the APS towards higher brilliance.

Table 1: APS Storage Ring Parameters in the Straight Section (for natural emittance $\epsilon = 8.2 \text{ nm}\cdot\text{rad}$)

| Function | Coupling | horizontal | vertical |
|------------------------|----------|------------|----------|
| β (m) | | 14.2 | 10.1 |
| σ (μ m) | 10% | 325 | 87 |
| σ' (μ rad) | 10% | 23 | 8.6 |
| σ (μ m) | 1% | 340 | 29 |
| σ' (μ rad) | 1% | 24 | 2.8 |
| σ (μ m) | 0.1% | 341 | 9 |
| σ' (μ rad) | 0.1% | 24 | 0.90 |

2 DIAGNOSTIC UNDULATOR

The undulator used in the APS diagnostics beamline was specially designed for divergence measurements [3] and has a narrow central cone of radiation and tight field tolerances.

2.1 Undulator Design

Table 2 lists the design parameters of the APS diagnostics undulator. It can be seen that the central cone of the first harmonic (2.6 μ rad) provides adequate resolution for measuring the baseline beam (8.6 μ rad at 10% vertical coupling) and the third harmonic (1.6 μ rad) for the case of 1% coupling (2.8 μ rad).

DISCLAIMER

**Portions of this document may be illegible
in electronic image products. Images are
produced from the best available original
document.**

DISCLAIMER

This report was prepared as an account of work sponsored by an agency of the United States Government. Neither the United States Government nor any agency thereof, nor any of their employees, makes any warranty, express or implied, or assumes any legal liability or responsibility for the accuracy, completeness, or usefulness of any information, apparatus, product, or process disclosed, or represents that its use would not infringe privately owned rights. Reference herein to any specific commercial product, process, or service by trade name, trademark, manufacturer, or otherwise does not necessarily constitute or imply its endorsement, recommendation, or favoring by the United States Government or any agency thereof. The views and opinions of authors expressed herein do not necessarily state or reflect those of the United States Government or any agency thereof.

Table 2: APS Diagnostics Undulator Design Parameters

| | |
|--|-----------------------|
| Period | 18 mm |
| Number of periods | 198 |
| Total length | 3.56 m |
| Center coordinate from beam waist, z_0 | 0.57 m |
| Minimum gap | 10.5 mm |
| Maximum peak magnetic field | 0.27 T |
| Maximum K-value | 0.45 |
| First harmonic photon energy ω_1 | 23.4 - 25.5 keV |
| Radiation cone angle at ω_1 | 2.7 - 2.6 μ rad |
| Third harmonic photon energy ω_3 | 70.2 - 75 keV |
| Radiation cone angle at ω_3 | 1.6 μ rad |
| Maximum peak power density | 116 kW/m ² |
| Maximum total power | 0.83 kW |
| Storage ring operation condition | 7 GeV / 100 mA |

2.2 Magnetic Field Measurements

The undulator was manufactured by STI Optronics. In order to realize the narrow radiation cone for beam diagnostics, the undulator's field errors were specified to be below those of other APS undulators. Table 3 summarizes the design specification for the field errors and the actually measured values at STI [4]. The field was also measured at the APS magnetic field measurement facility [5], with similar results.

Table 3: APS Diagnostics Undulator Field Errors

| Function | Spec | Actual |
|---|--------|--------------------|
| First horizontal field integral [g·cm] | 50 | 25 |
| First vertical field integral [g·cm] | 50 | 5.3 |
| Second horizontal field integral [g·cm ²] | 10^5 | 0.12×10^5 |
| Second vertical field integral [g·cm ²] | 10^5 | 0.06×10^5 |
| Integrated quadrupole field [g] | 50 | 38 |
| Integrated skew quadrupole field [g] | 50 | -16 |
| Integrated sextupole field [g/cm] | 200 | -17 |
| Integrated skew sextupole field [g/cm] | 100 | 3 |
| Integrated octupole field [g/cm ²] | 300 | -7 |
| Integrated skew octupole field [g/cm ²] | 50 | 14 |
| Relative transverse field roll-off | 0.1% | 0.02% |
| Magnetic field quality (fit residuals) | 0.5% | 0.4% |
| Rms phase error | 6° | 1.2° |
| RMS trajectory angle error | | |
| Horizontal [μ rad] | 1.0 | 0.9 |
| Vertical [μ rad] | 1.0 | 0.3 |
| RMS trajectory straightness | | |
| Horizontal [μ m] | 1.0 | 0.1 |
| Vertical [μ m] | 1.0 | 0.1 |

3 FRONT END

The front end of the diagnostics undulator beamline uses most components from the standard APS ID front ends [6]. However a number of special features were added to optimize the front end for beam diagnostics.

3.1 Beam Splitting Fixed Mask (FM1)

In addition to the undulator beam, the beamline is also designed to make use of the radiation from the bending magnet (designated as AM magnet in the APS nomenclature) just downstream of the insertion device to image the particle beam at the low dispersion region. The first fixed mask of the front end splits the beamline, and protects the downstream components from the missteered undulator beam. The design of the fixed mask utilizes grazing incidence in both horizontal and vertical planes to reduce the power density on the divider between the ID and AM beams. The aperture for the ID beam is 25 mm \times 6 mm. The aperture for the AM beam is 0.4 mm \times 0.4 mm, and is adjustable vertically.

3.2 Adjustable Pinhole Aperture for AM Source

An adjustable aperture formed by four independent blades is used as a pinhole for imaging the AM source. All blades are made of tungsten and controlled remotely via EPICS. The small aperture of the first fixed mask for the AM beam allows only 1 W of bending magnet radiation to pass through under normal operating conditions, which ensures the stable operation of the pinhole camera. It also allows only about 50 W of undulator beam to pass through when missteering occurs. This ensures the safety of the pinhole in such conditions.

3.3 Beryllium Windows

A pair of beryllium windows is used to separate the beamline from the storage ring vacuum, conforming to the APS vacuum policy. The window for the undulator beam employs a novel double concave shape for improved thermal conduction and higher flexural stiffness. A detailed thermal analysis is presented separately [7].

4 OPTICS AND DETECTOR

The divergence measurement was performed with a single crystal monochromator and an imaging detector using CdWO₄ scintillation crystal as a converter screen. Figure 2 shows the experimental setup.

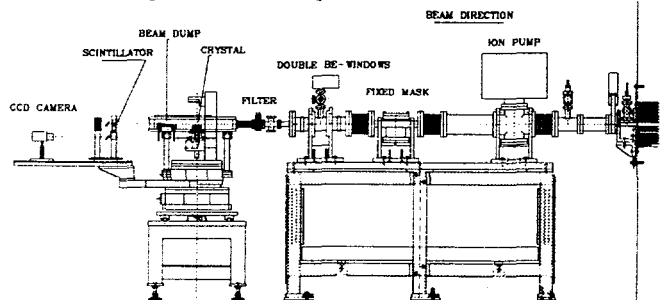


Figure 2: Schematics of the experimental setup for beam divergence measurement.

4.1 Monochromator

A Huber Goniometer is used as the base for the single crystal monochromator. The monochromator crystal, Ge(220), is clamped on a water-cooled copper block. The beam dump is made of GlidCop and is also enclosed in the monochromator chamber which is filled with helium. The monochromatic x-ray goes through an 80- μm aluminum window to reach the imaging detector located in the open air. Such an arrangement significantly reduces ozone generation by the white undulator beam.

4.2 Imaging Detector

The cross section of the monochromatic x-ray beam is imaged with a 0.3-mm-thick CdWO₄ scintillation crystal. A CCD camera with a C-mount photographic lens ($f=75$ mm) is used for the image acquisition. The pixel scale of the camera is calibrated with a grid pattern mounted on the background of the scintillator crystal. A Spiricon digitizer (120×120 pixels with 35 $\mu\text{m}/\text{pixel}$) is used to record the image.

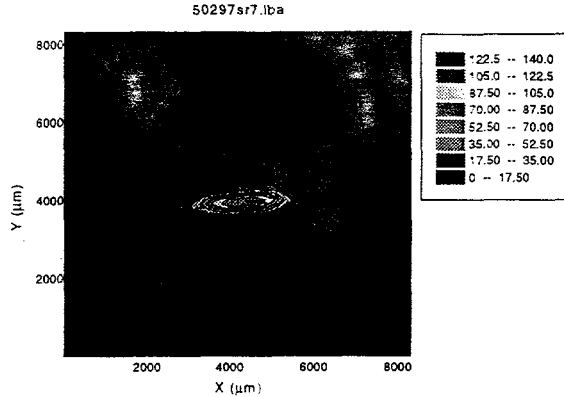


Figure 3: First image from the APS diagnostics undulator.

5 RESULTS

In the first experiment performed at the beamline on May 3, 1997, the undulator gap was set at 16.0 mm, with the first harmonic at 25.5 keV. The monochromator crystal angle was scanned to pass the maximum intensity point and to reach a minimum x-ray beam cross section. The photon energy was estimated to be around 25.7 keV. To simulate users' running conditions, the images of the x-ray beam were averaged every 8 frames (over 0.5 second) in the Spiricon, and five averaged images were recorded and examined to evaluate data consistency.

A typical beam image taken at a stored beam current of 65 mA is shown in Fig. 3. Table 4 shows the beam cross section and the inferred particle beam properties based on the design lattice functions. In these calculations, we have not considered the contribution of the imaging detector resolution, and its subtraction would likely further reduce

the measured beam emittance. The large error bars assigned to the beam parameters reflect largely the uncertainty of our knowledge about the lattice functions.

Table 4: APS Diagnostics Undulator Divergence Measurement (65 mA stored current)

| | |
|--|--|
| X-ray beam size ($\Sigma_x \times \Sigma_y$) | 674×164 (μm) ² |
| Partial emittance ($\epsilon_x \times \epsilon_y$) | 6.4×0.24 (nm·rad) |
| Total emittance (ϵ) | 6.6 ± 0.6 (nm·rad) |
| Vertical coupling (χ) | 0.037 ± 0.004 |
| e-beam size ($\sigma_x \times \sigma_y$) | 300×50 (μm) ² |
| e-beam divergence ($\sigma'_x \times \sigma'_y$) | 21×4.9 (μrad) ² |

6 SUMMARY

The APS diagnostics undulator has been commissioned and first results are used to characterize the storage ring beam. Using the design lattice functions, the measured particle beam size, divergence, and emittance are all within design specifications, which in turn translates to higher x-ray beam brilliance than the APS design goal.

7 ACKNOWLEDGEMENTS

We wish to thank I. Vasserman for his assistance in undulator field measurements; P. Den Hartog and E. Gluskin for their help in the undulator installation; M. Ramanathan, A. R. Passi, R. W. Nielsen, T. L. Kruy, J. Hawkins and N. Friedman for their help in the front end installation; and G. A. Decker and J. N. Galayda for their continued support for the project. This work was supported by U. S. Department of Energy, Office of Basic Energy Sciences under Contract No. W-31-109-ENG-38.

REFERENCES

- [1] E. Tarazona and P. Elleaume, "Emittance measurements at ESRF," *Rev. Sci. Instrum.* 66, 1995.
- [2] Z. Cai, R. J. Dejus, P. Den Hartog, Y. Feng, E. Gluskin, D. Haeffner, P. Illinski, B. Lai, D. Legnini, E. R. Moog, S. Shastr, E. Trakhtenberg, I. Vasserman, and W. Yun, "APS Undulator Radiation - First Results," *Rev. Sci. Instrum.* 67, (1996) CD ROM.
- [3] B. Yang and A. H. Lumpkin, "The Planned Photon Diagnostics Beamlines at the Advanced Photon Source," *BTW94*, AIP Conf. Proc. 333, Oct. 1994.
- [4] STI Optronics, "Magnetic Certification Data for U18, #14," 1996, unpublished.
- [5] L. Burkel, R. Dejus, J. Maines, J. O'Brien, J. Pflueger, and I. Vasserman, "The Insertion Device Magnetic Measurement Facility: Prototype and Operational Procedures," *ANL/APS/TB-12*, 1993.
- [6] D. Shu, and T. M. Kuzay, "General Layout Design for the Advanced Photon Source Beamline Front Ends," *Nucl. Instrum. Meth. A* 347, 1994.
- [7] I. C. Sheng, B. X. Yang, and S. Sharma, "Design and analysis of a Be window for the APS diagnostics undulator beamline," these proceedings.